Acta Crystallographica Section F
Structural Biology and Crystallization Communications
ISSN 1744-3091

Crystallization and preliminary X-ray diffraction analysis of the hyperthermophilic *Sulfolobus islandicus* lactonase

Guillaume Gotthard,[a] Julien Hiblot,[a] Mikael Elias[b] and Eric Chabrière[a]*

[a]Architecture et Fonction des Macromolécules Biologiques, CNRS–Aix Marseille Université, 13288 Marseille, France, and [b]Department of Biological Chemistry, Weizmann Institute of Science, Rehovot, Israel

Correspondence e-mail: eric.chabriere@afmb.univ-mrs.fr

Received 9 November 2010
Accepted 22 December 2010

Phosphotriesterase-like lactonases (PLLs) constitute an interesting family of enzymes that are of paramount interest in biotechnology with respect to their catalytic functions. As natural lactonases, they may act against pathogens such as *Pseudomonas aeruginosa* by shutting down their quorum-sensing system (quorum quenching) and thus decreasing pathogen virulence. Owing to their promiscuous phosphotriesterase activity, which can inactivate toxic organophosphorus compounds such as pesticides and nerve agents, they are equally appealing as potent bioscavengers. A new representative of the PLL family has been identified (*Sis*Pox) and its gene was cloned from the hyperthermophilic archeon *Sulfolobus islandicus*. Owing to its hyperthermostable architecture, *Sis*Pox appears to be a good candidate for engineering studies. Here, production, purification, crystallization conditions and data collection to 2.34 Å resolution are reported for this lactonase from the hyperthermophilic *S. islandicus*.

1. Introduction

*Sis*Pox is an enzyme from the archaeal organism *Sulfolobus islandicus*, which is found in extreme environments such as Yellowstone National Park in the USA and the Mutnovsky volcano in Kamchatka, Russia (Reno *et al.*, 2009). *Sis*Pox belongs to the phosphotriesterase-like lactonase (PLL) family of proteins (Afriat *et al.*, 2006) and displays 91% sequence identity to *Sso*Pox isolated from *Sulfolobus solfataricus* (Merone *et al.*, 2005). The PLL family contains several representatives, which include *Dr*OPH from *Deinoccocus radiodurans* (Hawwa, Larsen *et al.*, 2009), Gsp from *Geobacillus stearothermophilus* (Hawwa, Aikens *et al.*, 2009) and *Sso*Pox from *S. solfataricus* (Merone *et al.*, 2005). These proteins are natural quorum-quenching lactonases that exhibit promiscuous phosphotriesterase acitivity. This promiscuous activity might be a consequence of the divergence of PLLs from optimized phosphotriesterases (PTEs) (Afriat *et al.*, 2006) such as the PTE from *Pseudomonas diminuta* or OpdA found in *Agrobacterium radiobacter*.

All PLLs exhibit lactonase and phosphotriesterase activities, but to different extents. PLLs are natural lactonases that possess promiscuous weak phosphotriesterase activity (Afriat *et al.*, 2006). In contrast, the PTE from *P. diminuta* exhibits a phosphotriesterase activity towards the pesticide paraoxon which reaches the diffusion-limited rate of the substrate in water ($k_{cat}/K_M = 10^8\ M^{-1}\ s^{-1}$) (Omburo *et al.*, 1992) and possesses some lactonase activity (Draganov, 2010). Structural insights into this family of proteins are of great interest in order to understand the origin of the differences in substrate specificity that are observed between these two families.

The amidohydrolase superfamily (Seibert & Raushel, 2005) that encompasses PLLs and PTEs exhibits a classical $(\alpha/\beta)_8$-barrel fold with two divalent metal cations in the active site, which is located at the C-terminus of the barrel. The catalytic mechanism involves a nucleophilic attack by a water molecule activated as a hydroxide ion by the bimetallic centre (Elias *et al.*, 2008). The hydrolysis of phosphotriester substrates is performed *via* a pentacoordinate transition

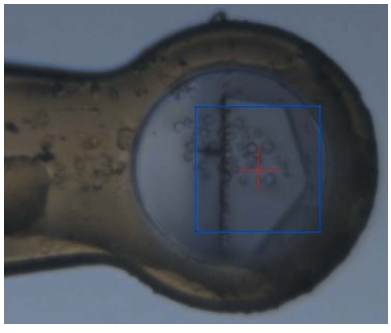

state (Elias *et al.*, 2008). The PLL active site presents three subsites that are remarkably well adapted for lactone binding: a small subsite, a large subsite and a hydrophobic channel (Elias *et al.*, 2008; Del Vecchio *et al.*, 2009). The aliphatic chain of the lactones binds within the hydrophobic channel, the large subsite adapts the carbonyl group of the chain and the small subsite positions the lactone ring. During catalysis, the bridging hydroxide ion attacks the carbonyl carbon of the lactone ring, forming a tetrahedral transition state. The ability of PLLs, including *Sis*Pox, to hydrolyze lactones, and especially acyl-homoserine lactones (AHLs), is interesting. Indeed, several pathogens use AHLs to communicate and to coordinate the transcription of some genes (Popat *et al.*, 2008). This communication behaviour is known as a quorum-sensing system (QS). The perturbation of bacterial communication using lactonases, a process that is known as quorum quenching (QQ), is seen as a potent antibiotic strategy (Reimmann *et al.*, 2002). Moreover, the presence of QQ lactonases in archaea raises the question of the utilization of QS by these organisms (Elias *et al.*, 2008). Another hypothesis would involve the advantage provided by such a QQ enzyme in controlling the QS of concurrent organisms in the natural biotope.

*Sis*Pox, like *Sso*Pox, also exhibits phosphotriesterase activity (unpublished data). Such enzymes are able to hydrolyze neurotoxic organophosphate (OP) pesticides, as well as OP nerve agents such as sarin, soman and VX (Raushel, 2002). Current methods for removal of these compounds, which include bleach treatment and incineration, are slow, expensive and harmful to the environment. Therefore, enzymes that are able to hydrolyze these compounds are appealing (LeJeune *et al.*, 1998). Because of their intrinsic thermal stability, enzymes such as *Sis*Pox represent interesting candidates for the engineering of an OP bioscavenger (Demirjian *et al.*, 2001).

In this report, we describe the purification, crystallization, data collection and preliminary X-ray diffraction analysis of *Sis*Pox, a new member of the PLL family.

2. Expression and purification

The *sispox* gene was synthesized with an N-terminal linker containing a Strep-tag and a TEV cleavage site (GeneArt, Germany). The construct was subcloned in the plasmid pET22b (Novagen). The protein was produced in *Escherichia coli* Rosetta (DE3) pLysS strain (Invitrogen).

Protein production was performed in 8 l ZYP medium (Studier, 2005) (100 µg ml^{-1} ampicillin, 34 µg ml^{-1} chloramphenicol) inoculated with an overnight pre-culture at a 1:20 ratio. Cultures were grown at 310 K until they reached an $OD_{600\,nm}$ of 1.5. Induction of the protein took place on consumption of the lactose in the ZYP medium with the addition of 0.2 m*M* $CoCl_2$ and a temperature transition to 298 K for 20 h. Cells were harvested by centrifugation (3000*g*, 277 K, 10 min), resuspended in lysis buffer (50 m*M* HEPES pH 8, 150 m*M* NaCl, 0.2 m*M* $CoCl_2$, 0.25 mg ml^{-1} lysozyme, 10 µg ml^{-1} DNAse, 20 m*M* $MgSO_4$ and 0.1 m*M* PMSF) and stored at 193 K overnight. Suspended frozen cells were thawed at 310 K for 15 min and disrupted by three 30 s sonication steps (Branson Sonifier 450; 80% intensity and microtip limit of 8). Cell debris was removed by centrifugation (12 000*g*, 277 K, 30 min).

The crude extracts clarified by centrifugation were charged onto a StrepTrap HP chromatography column (GE Healthcare). The bound proteins on the column were eluted by competition with elution buffer (50 m*M* HEPES pH 8, 150 m*M* NaCl, 0.2 m*M*$CoCl_2$, 4 m*M* desthiobiotin). The eluted protein was cleaved by TEV protease (van den Berg *et al.*, 2006) at a 1:20(*w*:*w*) ratio during overnight incubation at 303 K. Precipitated TEV protease was harvested by centrifugation (12 000*g*, 277 K, 30 min). The sample was reloaded onto a StrepTrap chromatography column (GE Healthcare) and cleaved *Sis*Pox was obtained in the flowthrough fraction. The protein obtained was subsequently loaded onto a size-exclusion chromatography column (Superdex 75 16/60, GE Healthcare) and fractions containing pure protein were pooled. About 5 mg protein was obtained from 8 l culture medium. The purity of the protein was checked by 15% SDS–PAGE separation under reducing conditions at 250 V for 40 min. The gel was stained using the Coomassie Blue method (0.3% Coomassie Blue, 0.2 *M* citric acid) and destained in water.

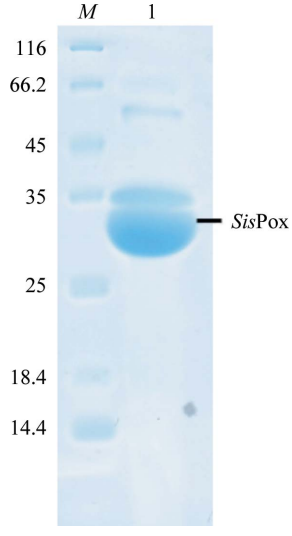

Figure 1
15% SDS–PAGE of the *Sis*Pox protein. Lane *M*, molecular-weight markers (Euromedex 06U-0511; labelled in kDa). Lane 2, 8 µl *Sis*Pox protein at 5 mg ml^{-1}.

3. Crystallization

*Sis*Pox was concentrated to 5.44 mg ml^{-1} using a centrifugation device (Amicon Ultra centrifugal units with 10 kDa cutoff; Millipore, Carrigtwohill, County Cork, Ireland) and its purity was checked on SDS–PAGE (Fig. 1). Crystallization was performed using a sitting-drop vapour-diffusion setup in 96-well plates at 293 K. The best hit was obtained using the commercial screens Wizard I and II (Emerald BioSystems) in a condition consisting of 2 *M* ammonium sulfate,

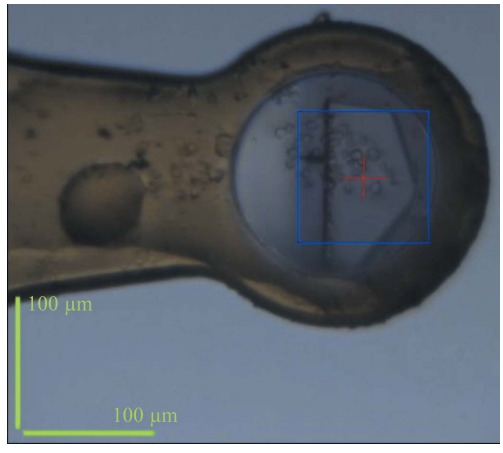

Figure 2
A crystal of the *Sis*Pox protein mounted in a MiTeGen MicroLoop.

0.1 *M* Tris pH 7.0 and 0.2 *M* lithium sulfate. A single crystal appeared after one month at 293 K in a drop containing a 3:1 protein:reservoir ratio (Fig. 2).

4. Data collection

A cryoprotectant solution consisting of the crystallization solution supplemented with 20%(*v*/*v*) glycerol was added to the drop in order to exchange the solution containing the crystal. The crystal was mounted on a MicroLoop (MiTeGen) and flash-frozen in liquid nitrogen at 100 K. X-ray diffraction intensities were collected on the ID14-EH1 beamline at the ESRF (Grenoble, France) using a wavelength of 0.933 Å and an ADSC Quantum Q210 detector with 12 s exposures. Diffraction data were collected from 92 images using the oscillation method; individual frames consisted of 1.0° oscillation steps over a range of 92° (Fig. 3).

5. Results and conclusions

X-ray diffraction data were integrated, scaled and merged using the *XDS* program (Kabsch, 2010) and the *CCP*4 program suite (Collaborative Computational Project, Number 4, 1994). The best result with the highest symmetry suggested that the *Sis*Pox crystal belonged to the hexagonal space group $P6_222$, with unit-cell parameters $a = 47.8$, $b = 47.8$, $c = 239.5$ Å (quality of fit = 6.0). The $R_{\rm merge}$ of 7.1% and the multiplicity of 9.16 confirmed that symmetry operators were present: a sixfold axis (z) and two twofold axes (x, y). Nevertheless, the Matthews coefficient ($V_{\rm M}$; Matthews, 1968) calculated for a monomer of *Sis*Pox (35.6 kDa) corresponded to a very low value of 1.11 Å^3 Da^{-1} with an impossible solvent content of −11.2% (calculated with http://csb.wfu.edu/tools/vmcalc/vm.html). Data quality was assessed using *phenix.xtriage* (Zwart *et al.*, 2005) from the *PHENIX* refinement-program suite (Adams *et al.*, 2002). An *L* test was performed on the data and the results (Fig. 4) suggested possible merohedral twinning. Although a molecular-replacement solution was unlikely in this space group, it was tested with *Phaser* (McCoy *et al.*, 2007) using the structure of *Sso*Pox as a model (PDB code 2vc5; Elias *et al.*, 2007). Robust solutions for the rotation and translation functions (RFZ = 9.5 and TFZ = 12.4) were found, but the solution was rejected owing to the large number of clashes (143). All of these results suggested supplementary symmetry arising from twinning.

The data were reprocessed in $P3_221$ using *XDS* (Table 1). This space group contains fewer asymmetric units in the unit cell and was of the highest symmetry that retains coherency in term of $V_{\rm M}$. The $V_{\rm M}$ and solvent content were calculated and gave more typical values (2.21 Å^3 Da^{-1} and 44.4%, respectively, with one molecule in the asymmetric unit). A *phenix.xtriage* analysis estimated the twin fraction to be 0.487 (*H* test). A twofold axis (z) arising from the twinning and the twin law ($-h$, $-k$, l) were proposed. The twin operator explained how $P3_221$ could be confused with $P6_222$.

Molecular replacement was performed with *Phaser* using the *Sso*Pox structure as a model (PDB code 2vc5). One robust solution was found with one molecule in the asymmetric unit (RFZ = 6.2 and TFZ = 12.7). The electron-density map was calculated with model phases obtained from molecular replacement, but the best solution

Table 1
Diffraction data collected on the ID14-EH1 beamline at the ESRF, Grenoble, France.

Values in parentheses are for the highest resolution shell.

Wavelength (Å)	0.9334	
Detector	ADSC Quantum Q210	
Crystal-to-detector distance (mm)	262.50	
No. of crystals	1	
Temperature (K)	100	
Exposure per frame (s)	12	
Oscillation (°)	1	
Total rotation range (°)	92	
Resolution (Å)	79.71–2.34 (2.50–2.34)	
Space group	$P3_221$	$P6_222$
Unit-cell parameters (Å, °)	a = 47.8, b = 47.8, c = 239.5, α = 90.0, β = 90.0, γ = 120.0	a = 47.8, b = 47.8, c = 239.5, α = 90.0, β = 90.0, γ = 120.0
No. of observed reflections	69183 (8477)	69274 (8494)
No. of unique reflections	14077 (2381)	7560 (1287)
Completeness (%)	98.6 (95.1)	99.6 (98.3)
$R_{\rm merge}$† (%)	9.4 (60.9)	7.1 (48.4)
$R_{\rm meas}$‡ (%)	5.8 (47.2)	6.0 (48.1)
$\langle I/\sigma(I)\rangle$	20.13 (2.56)	26.44 (3.42)
Multiplicity	4.91 (3.56)	9.16 (6.60)
Mosaicity (°)	0.134	0.134

† $R_{\rm merge} = \sum_{hkl}\sum_i |I_i(hkl) - \langle I(hkl)\rangle| / \sum_{hkl}\sum_i I_i(hkl)$. ‡ $R_{\rm meas} = \sum_{hkl}[N/(N-1)]^{1/2} \times \sum_i |I_i(hkl) - \langle I(hkl)\rangle| / \sum_{hkl}\sum_i I_i(hkl)$.

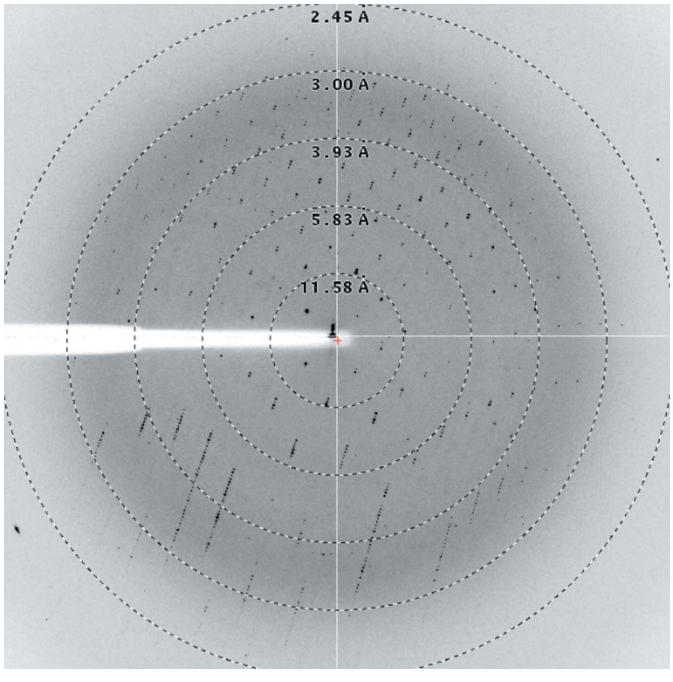

Figure 3
A diffraction pattern from a crystal of *Sis*Pox. The edge of the frame is at 2.5 Å resolution.

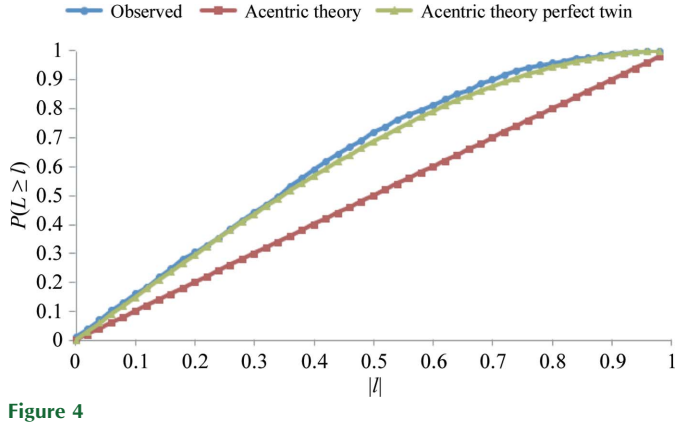

Figure 4
The *L* test indicates that the intensity statistics are significantly different from those that would be expected for good to reasonable untwinned data.

was not certain because of the twinning (R factor of 55% after molecular replacement). The two metal cations (iron and cobalt) in the active site were then removed from the model and the maps were recalculated. Two strong peaks (5.7σ and 8σ, respectively) corresponding to the two metal cations were clearly visible in the $F_{obs} - F_{calc}$ map, showing that the molecular-replacement solution was correct. Use of the twin option in *REFMAC*5 (Vagin *et al.*, 2004) allowed us to obtain untwinned maps that were of sufficient quality for model building. Manual model improvement was performed using *Coot* (Emsley & Cowtan, 2004). Refinement of the structure of *Sis*Pox at 2.34 Å resolution and its interpretation are in progress.

This research was supported by grants to EC from the Délégation Générale pour l'Armement (DGA) (REI#09C7002) and from CNRS. GG is a doctoral fellow supported by the DGA. ME is a fellow supported by the IEF Marie Curie program (grant No. 252836). We thank Dr Alain Dautant for fruitful discussions about twinning.

References

Adams, P. D., Grosse-Kunstleve, R. W., Hung, L.-W., Ioerger, T. R., McCoy, A. J., Moriarty, N. W., Read, R. J., Sacchettini, J. C., Sauter, N. K. & Terwilliger, T. C. (2002). *Acta Cryst.* D**58**, 1948–1954.
Afriat, L., Roodveldt, C., Manco, G. & Tawfik, D. S. (2006). *Biochemistry*, **45**, 13677–13686.
Berg, S. van den, Löfdahl, P. A., Härd, T. & Berglund, H. (2006). *J. Biotechnol.* **121**, 291–298.
Collaborative Computational Project, Number 4 (1994). *Acta Cryst.* D**50**, 760–763.
Del Vecchio, P., Elias, M., Merone, L., Graziano, G., Dupuy, J., Mandrich, L., Carullo, P., Fournier, B., Rochu, D., Rossi, M., Masson, P., Chabriere, E. & Manco, G. (2009). *Extremophiles*, **13**, 461–470.
Demirjian, D. C., Morís-Varas, F. & Cassidy, C. S. (2001). *Curr. Opin. Chem. Biol.* **5**, 144–151.
Draganov, D. I. (2010). *Chem. Biol. Interact.* **187**, 370–372.
Elias, M., Dupuy, J., Merone, L., Lecomte, C., Rossi, M., Masson, P., Manco, G. & Chabriere, E. (2007). *Acta Cryst.* F**63**, 553–555.
Elias, M., Dupuy, J., Merone, L., Mandrich, L., Porzio, E., Moniot, S., Rochu, D., Lecomte, C., Rossi, M., Masson, P., Manco, G. & Chabrière, E. (2008). *J. Mol. Biol.* **379**, 1017–1028.
Emsley, P. & Cowtan, K. (2004). *Acta Cryst.* D**60**, 2126–2132.
Hawwa, R., Aikens, J., Turner, R. J., Santarsiero, B. D. & Mesecar, A. D. (2009). *Arch. Biochem. Biophys.* **488**, 109–120.
Hawwa, R., Larsen, S. D., Ratia, K. & Mesecar, A. D. (2009). *J. Mol. Biol.* **393**, 36–57.
Kabsch, W. (2010). *Acta Cryst.* D**66**, 125–132.
LeJeune, K. E., Wild, J. R. & Russell, A. J. (1998). *Nature (London)*, **395**, 27–28.
McCoy, A. J., Grosse-Kunstleve, R. W., Adams, P. D., Winn, M. D., Storoni, L. C. & Read, R. J. (2007). *J. Appl. Cryst.* **40**, 658–674.
Matthews, B. W. (1968). *J. Mol. Biol.* **33**, 491–497.
Merone, L., Mandrich, L., Rossi, M. & Manco, G. (2005). *Extremophiles*, **9**, 297–305.
Omburo, G. A., Kuo, J. M., Mullins, L. S. & Raushel, F. M. (1992). *J. Biol. Chem.* **267**, 13278–13283.
Popat, R., Crusz, S. A. & Diggle, S. P. (2008). *Br. Med. Bull.* **87**, 63–75.
Raushel, F. M. (2002). *Curr. Opin. Microbiol.* **5**, 288–295.
Reimmann, C., Ginet, N., Michel, L., Keel, C., Michaux, P., Krishnapillai, V., Zala, M., Heurlier, K., Triandafillu, K., Harms, H., Défago, G. & Haas, D. (2002). *Microbiology*, **148**, 923–932.
Reno, M. L., Held, N. L., Fields, C. J., Burke, P. V. & Whitaker, R. J. (2009). *Proc. Natl Acad. Sci. USA*, **106**, 8605–8610.
Seibert, C. M. & Raushel, F. M. (2005). *Biochemistry*, **44**, 6383–6391.
Studier, F. W. (2005). *Protein Expr. Purif.* **41**, 207–234.
Vagin, A. A., Steiner, R. A., Lebedev, A. A., Potterton, L., McNicholas, S., Long, F. & Murshudov, G. N. (2004). *Acta Cryst.* D**60**, 2184–2195.
Zwart, P. H., Grosse-Kunstleve, R. W. & Adams, P. D. (2005). *CCP4 Newsl.* **43**, contribution 7.